Nuclei Charge measurement with the AMS-02 Silicon Tracker

G. Ambrosi,[1] **P. Azzarello,**[2] **R. Battiston,**[3,4,a] **J. Bazo,**[1,b] **B. Bertucci,**[1,5] **E. Choumilov,**[6] **V. Choutko,**[6] **M. Crispoltoni,**[1,5] **C. Delgado,**[7] **M. Duranti,**[1,5] **F. Donnini,**[1,5] **D. D'Urso,**[1,c] **E. Fiandrini,**[1,5] **V. Formato,**[1,11] **M. Graziani,**[1,5] **M. Habiby,**[2] **S. Haino,**[8] **M. Ionica,**[1] **K. Kanishchev,**[3,4,11] **F. Nozzoli,**[1,c] **A. Oliva,**[7] **M. Paniccia,**[2] **C. Pizzolotto,**[1,c] **M. Pohl,**[2] **X. Qin,**[1,d] **D. Rapin,**[2] **P. Saouter,**[2] **N. Tomassetti,**[9] **V. Vitale,**[1,c] **S. Vitillo**[*,2] **X.Wu,**[2] **Z. Zhang,**[10] **P. Zuccon**[6]

[1]*INFN Sezione di Perugia, I-06100 Perugia, Italy*
[2]*DPNC, Université de Genève, CH-1211 Genève 4, Switzerland*
[3]*INFN TIFPA, I-38123 Povo, Trento, Italy*
[4]*Università di Trento, I-38123 Povo, Trento, Italy*
[5]*Università di Perugia, I-06100 Perugia, Italy*
[6]*Massachusetts Institute of Technology (MIT), Cambridge, Massachusetts 02139, USA*
[7]*Centro de Investigaciones Energéticas, Medioambientales y Tecnológicas (CIEMAT), E-28040 Madrid, Spain*
[8]*Institute of Physics, Academia Sinica, Nankang, Taipei, 11529, Taiwan*
[9]*LPSC, CNRS/IN2P3 and Université Grenoble-Alpes, F-38026 Grenoble, France*
[10]*Sun Yat-Sen University (SYSU), Guangzhou, 510275, China*
[11]*European Organization for Nuclear Research (CERN), CH-1211 Geneva 23, Switzerland*
[a]*Also at ASI, I-00133 Roma, Italy.*
[b]*Present address: Departamento de Ciencias, Pontifica Universidad Católica del Perú (PUCP), Lima 32, Peru.*
[c]*Also at ASI Science Data Center (ASDC), I-00133 Roma, Italy.*
[d]*Also at Shandong University (SDU), Jinan, Shandong, 250100, China.*
E-mail: stefania.vitillo@cern.ch

The Alpha Magnetic Spectrometer (AMS-02) is an astroparticle physics detector that has been installed on the International Space Station (ISS) in May 2011. The purpose of the experiment is to study with unprecedented precision and statistics cosmic-ray particles in an energy range from 0.5 GeV to few TeV. The AMS-02 Tracker system accurately determines the trajectory and absolute charge (Z) of cosmic rays by multiple measurements of the coordinates in nine layers of double-sided silicon micro-strip detectors. Given the high dynamic range of the front-end electronics, nuclei from hydrogen up to iron and above can be identified. The charge resolution could be naturally degraded by a number of detector effects that need to be carefully accounted for. In this contribution we describe the procedure that has been used to accurately calibrate the Tracker response. Finally we will discuss the Tracker calibration stability with time.

---

[*]Speaker.

1. The Alpha Magnetic Spectrometer AMS-02

The Alpha Magnetic Spectrometer is an astroparticle detector operating as an external module on the International Space Station since May 2011 that can perform accurate measurements of the spectra of charged cosmic rays from 0.5 to few TeV energy. The absolute fluxes of different chemical species, as well as their relative abundance, will help to improve models of acceleration and propagation of cosmic rays in the galaxy and help addressing fundamental questions like the search for dark matter and antimatter. As depicted in Fig.1, the core of the instrument is actually a permanent magnet generating a field of about ≈ 0.14 T within a cylindrical shaped volume (diameter and height ≈ 1 m) surrounding a precision tracking device. Seven layers of silicon detectors inside the magnet volume (Inner Tracker) and two layers outside the field volume allow to reconstruct the tracks of charged particles and measure the particle magnetic rigidity $R = pc/Ze$. The Tracker measures with an excellent resolution the magnitude of the charge of the traversing particle, offering up to nine independent measurements (nine layers in total) of the specific energy loss dE/dx. At both ends of the magnet two segmented scintillator planes are placed to measure the velocity of charged particles (ToF). The AntiCoincidence scintillator Counter (ACC) is a barrel of scintillation counters surrounding the Inner Tracker and providing a veto signal against particles entering the detector side ways. The Ring Imaging Čherenkov (RICH) is located below the magnet and measures the particle velocity and charge. The Transition Radiation Detector (TRD), placed on top of AMS ensures e/p separation and the Electromagnetic CALorimeter (ECAL), at the bottom of AMS allows an accurate discrimination between electromagnetic particles and hadrons and serving excellent energy measurement for leptons and photons.
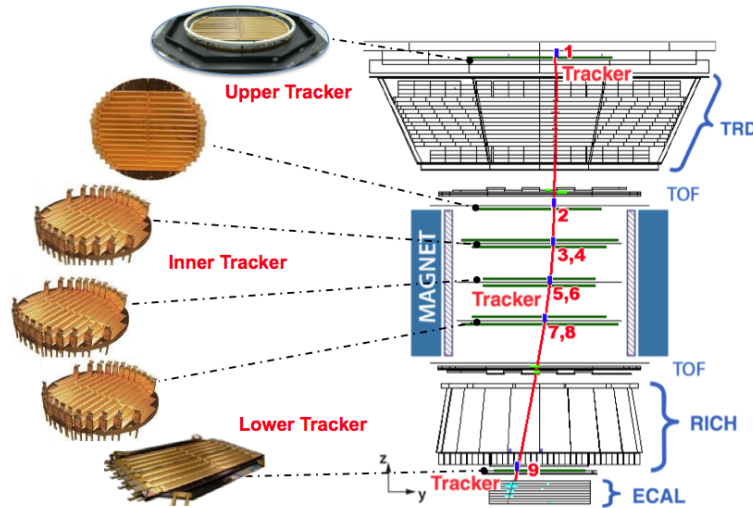

Figure 1: Display of the main subdetectors composing AMS-02, presented in the bending $(y - z)$ plane of the magnetic field. The red line corresponds to a measured low energy proton [1].

2. The Silicon Tracker

2.1 The Detector

The AMS-02 Tracker is composed of 2284 double-sided silicon micro-strip sensors, with dimensions $\sim 72 \times 41 \times 0.3$ mm^3, assembled in basic functional elements called *ladders*. Each ladder is composed of 9 to 15 sensors, for a total of 192 ladders and a sensitive area of 6.75 m^2. Each face of a sensor is implanted with strips running in orthogonal directions, providing a bidimensional measurement of the particle's position. The junction side (or p-side) is composed of 14 μm wide p$^+$ doped strips, with an implantation pitch of 27.5 μm; the opposite ohmic side (the n-side) has 40 μm wide strips, with a larger implantation pitch of 104 μm. The front-end hybrid design is based on a high dynamic range 64 channel chip developed on the basis of the VA and Viking chips [2]. A total of 10(6) VA chips are used to read the signals from the p(n) sides. Details of the tracker design and the construction of sensors and ladders can be found in [3]. When a particle traverses a silicon sensor, electron-hole pairs are created along the particle trajectory. Due to the electric field in the depleted area, electron and holes migrate to opposite sides. The opposite sign of the collected signals has an impact on the VA performances which are therefore different on the two sides and implies separated calibrations.

The deposited ionization energy in a silicon sensor is proportional to the square of the particle charge ($dE/dx \propto Z^2$), therefore allowing to distinguish different nuclei species. The analog readout and the high dynamic range of the front-end electronics of the Tracker ladders allow to identify nuclei from hydrogen up to iron and above. In the construction phase of the detector, a limited number of ladders have been exposed to several particle beams in order to evaluate their performances, in terms of position resolution and charge identification capabilities [4].

2.2 Charge Measurement

The ionization energy lost in a silicon sensor is collected by a cluster of adjacent read-out strips. The cluster amplitude, which is proportional to the energy deposited by the particle, is defined as the sum of each single cluster strip signal. The ADC values of the readout strips include several contributions: a constant offset (pedestal), a common noise component, the strip noise and the signal corresponding to the charge accumulated on the strip due to the passage of a particle. The cluster amplitude depends on the impact position of the particle on the sensor and on its impact angle (see Fig.2).

This dependence is a consequence of a loss of collection efficiency when a particle traverses the sensor surface in between two readout strips, while the maximum charge collection efficiency appears when the particle impacts vertically on a readout strip. At higher inclinations, the signal tends to be distributed to a larger number of strips which partially compensates the loss of collection and attenuates the effect. The total effect can amount to differences up to more than 30% for the lighter nuclei ($Z < 6$). As the charge increases, the deposited energy is collected by an increasing number of readout strips and the effect tends to decrease.

3. Charge Equalization

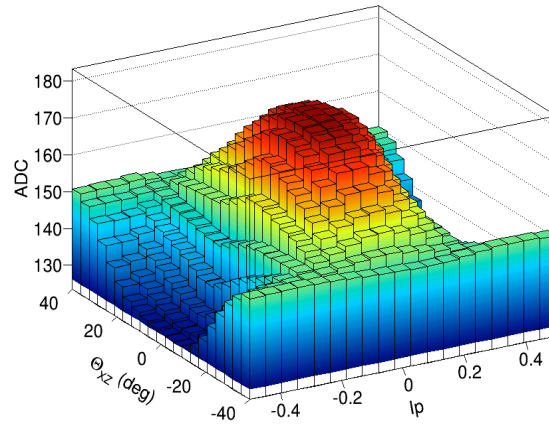The Tracker charge resolution is degraded by a number of effects, due to the response of the

Figure 2: Dependence of the signal of a cosmic particle from the impact point and impact angle of the particle for a selected sample of helium nuclei. The maximum of collection efficiency appears when the particle traverses at vertical incidence a readout strip ($IP = 0$ and $\theta_{xz} = 0$) [5].

detector, that need to be carefully taken into account and corrected for. In-flight calibration of the Tracker is done using the statistics accumulated over two years of operation. This is obtained using the characteristic energy deposition signature of the most abundant nuclei.

3.1 Charge Selection

To study the response of the electronics as a function of the charge we selected a sample of nuclei and computed the truncated mean (S_T) of cluster signals S_i belonging to a reconstructed particle track in the tracker:

$$S_T = \frac{\sum_{i=1}^{n} S_1 - S_{max}}{n - 1} \tag{3.1}$$

The square root of the truncated mean calculation is used for its direct proportionality to the charge of the particle ($\sqrt{S_T} \propto Z$). Fig.3 gives an overview of the selection. We used a data sample where the contribution of charge 1 particles has been prescaled by a factor 1000, given the overwhelming natural abundance of protons. The truncated mean is fitted with a multigaussian function from which we extract single gaussian contributions around the peak values for the different nuclei. This definition ensures a contamination from the Z + 1 and Z - 1 samples lower than 1% up to oxygen at 68% selection efficiency.

3.2 VA equalization

We first corrected for differences in the response of the VA chips. We fit the energy loss distributions using a Landau convoluted with a Gaussian noise function from which we extract the Most Probable Value (MPV) to characterize the peak position of the distribution. For each one of the 3072 VA units (10 are on p-side (640 channels) and 384 on the n-side of the silicon junction) , the MPV values are extracted for hydrogen, helium and carbon. We used a sample of known high quality VAs to compute reference MPV values to which all the VA responses are equalized. Due
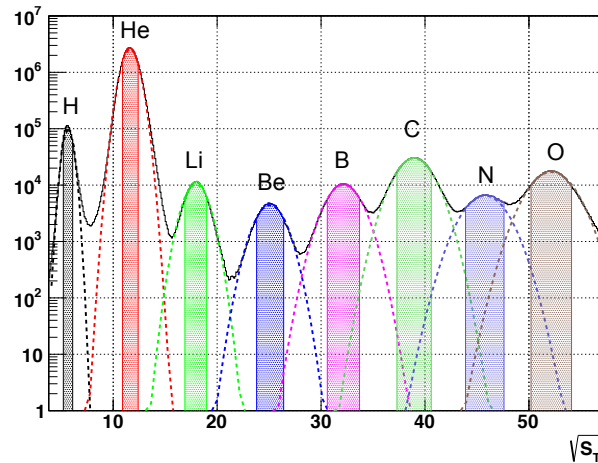
Figure 3: The n-side truncated mean distribution for a sample where the contribution of charge 1 particles has been prescaled by a factor 1000. The peaks of nuclei up to oxygen are clearly visible. The super-imposed gaussian functions are constructed from the parameters resulting from a multigaussian fit to the distribution.

to the loss of collection efficiency in regions between readout strips, the analysis is performed in two separated readout regions to avoid any bias in the signal estimation. The dependence with the inclination of the particle is neglected in order to save statistics. We further imposed a cut on the β of the particle to be greater than 0.97 to remove the low energy dependence of energy loss in matter (see Fig.4).

3.3 Charge Loss Correction

Once the VA responses are equalized, we combined the statistics of the p and n-side VAs to produce 3-dimensional description plots of the type of Fig.2 for the different nuclei and for each sensor side. The resolution of this procedure depends on the relative abundances of the different nuclei. Where statistics was sufficient, we tested with the Landau-Gaussian function to the signal distribution in each bin of impact parameter and inclination. With the resulting MPV values, maps of the charge loss effect are created for each nuclei. The equalization was applied to ADC signals by searching for the closest 3-dimensional point in the stored maps. When a point was missing in a given map, the correction algorithm interpolates between the information of the next closest maps. In the process of correcting for this effect, the ADC scale of the deposited energy measurement is converted to nuclear charge units.

3.4 Energy Dependence

The deposited energy presents a dependence with the energy of the particle, following the Bethe-Bloch formula. The observed dependence for a proton sample measured with the AMS Silicon Tracker is shown in Fig.4.

We describe the energy dependence using the universal $\beta\gamma$ parameter, corresponding to the momentum over mass value of the particle. This parameter can be estimated directly from the ToF β measurement and indirectly from the Tracker reconstructed rigidity (R).
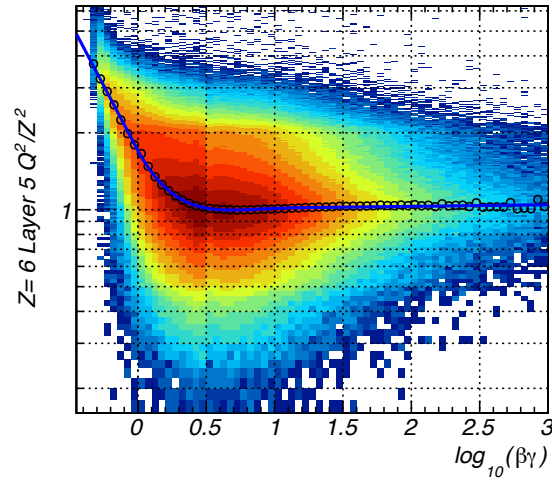
Figure 4: Carbon nuclei ionisation energy loss in a single layer as a function of $\beta\gamma$.

The rigidity estimation is used for the high energy description. To account for the additional energy lost by the particle while traversing the AMS detector material, the correction is implemented for each layer and each sensor side, and a specific parametrization is derived for each nuclei.

3.5 Final Equalization

After correcting for the main effects affecting the charge resolution of the tracker measurement, we observe significant residual differences in the VA chips responses, starting around the CNO group on the p-side, and above magnesium for the n-side. This is understood in terms of a change of slope at different points in the response curve of both sides. We fitted the signal distribution for each single VA with no restriction on impact regions nor on energy since we have corrected for these effects. Without these limitations, the accumulated statistics until May 2013 was enough to extract MPV values for each single nucleus up to iron, and perform the calibration to the unit charge value.

4. Charge Identification Performances

Fig.5 (left plot) shows the distributions of events in the p (blue) and n-side (red) charge measurements before and after all the calibration steps are applied.

The improvement in resolution is most significant for charges up to magnesium, where the n-side response starts saturating, while for the p-side, a non-linear region is achieved around the CNO group [4]. The two measurements can be combined together using a weighted sum, depending on the number of points used in the truncated mean computation. The final combined estimator is shown in Fig.5 (right plot) over the full range of charges. Nuclei up to silicon (Z=14) can clearly be separated. Above, nuclei with even charge number can also be distinguished. The iron peak itself is clearly visible due to its natural higher abundance in cosmic nuclei. For the combined
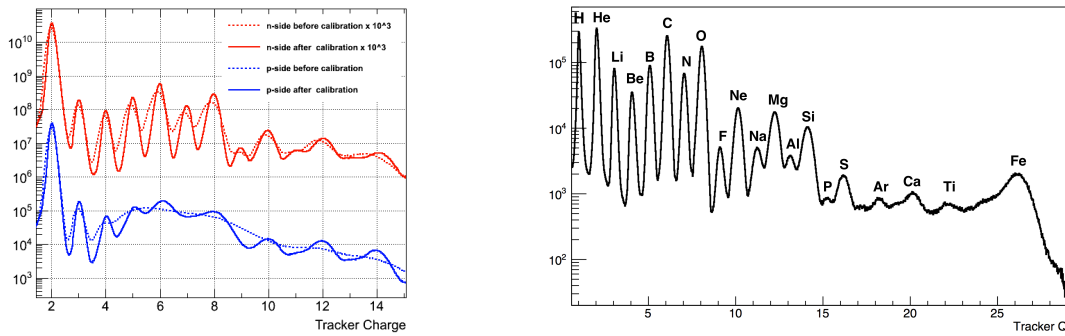
Figure 5: Left: improvement in the tracker charge measurement after applying the calibration, for the n-side (red) and p-side (blue) measurements. Right: final tracker charge distribution of events for the combined p and n-side measurements.

measurement, we reach a resolution of 0.1 charge units (c.u.) for carbon and lower than 0.3 c.u. up to silicon [5].

5. Time Stability

We investigated the potential dependence of the calibration procedure with time. We studied the stability of the final Tracker estimator in function of time for two separate time periods. The first one, from May 2011 to May 2013, corresponds to the data sample used to perform the calibration. The second sample corresponds to an additional six months of data acquired after May 2013. Fig.6 summarizes the results for hydrogen (upper plots) and carbon nuclei (bottom plots). The left plot shows the normalized tracker charge estimator as a function of time where the black points correspond to the profile (average charge value for each time bin) of the underlying 2-dimensional distribution. The right plot shows the projected profile for the two distinct time periods described above. One can observe that the RMS of both distributions are well below 1%. For nuclei up to silicon, no significant time dependences have been found.

6. Conclusions

We presented a procedure to improve the charge identification capability of the AMS-02 Silicon Tracker. After correcting for the most relevant effects degrading the charge measurement, we reach an excellent overall charge separation power with a misidentification probability for carbon lower than 10^{-3}. The stability of the charge measurement of the Tracker with time was tested using a sample of data included in the calibration and a sample of data not included. No significant time dependences are found for both samples.
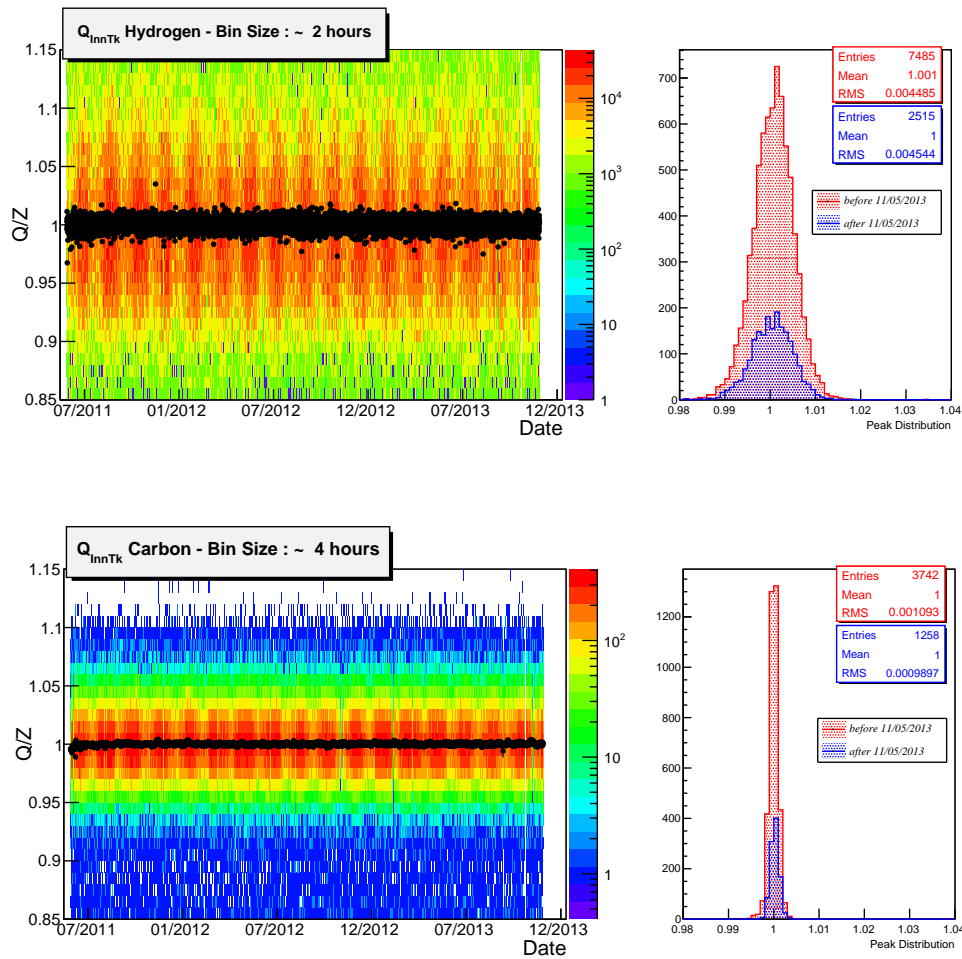
Acknowledgements

Figure 6: Left: normalized tracker charge estimator as a function of time for hydrogen and carbon nuclei. Right: distribution of average Q/Z values for the two detecting periods before and after 11/05/2013.

References

[1] P. Saouter, *Operation and Performance of AMS-02 Silicon Tracker* in proceedings of *The 23rd International Workshop on Vertex Detectors*, `PoS(Vertex2014)030` 2014

[2] E.Nygard et al., *CMOS low noise amplifier for microstrip readout Design and results*, Nucl. Instr. and Meth. A301 (1991) 506

[3] J.Alcaraz et al., *The Alpha Magnetic Spectrometer Silicon Tracker: Performance results with protons and helium nuclei*, Nucl. Instr. and Meth. A 593 (2008) 378

[4] B. Alpat and al., *Charge determination of nuclei with the AMS-02 silicon tracker*, Nucl. Instr. and Meth. A 540 (2005) 121-130

[5] P. Saouter et al., *Nuclear Charge Measurement with the AMS-02 Silicon Tracker*, Proceeding for 33rd International Cosmic Rays Conference (2013)